

## Supporting information

### Chemical Ordering in Bimetallic FeCo Nanoparticles : from a direct chemical synthesis to application as efficient high frequency magnetic material

Cyril Garnero,<sup>1</sup> Mathieu Lepasant,<sup>1</sup> Cécile Garcia-Marcelot,<sup>1,2</sup> Yooleemi Shin,<sup>3,4</sup> Christian Meny,<sup>3</sup> Pierre Farger,<sup>1-2</sup> Bénédicte Warot-Fonrose,<sup>2</sup> Raul Arenal,<sup>5,6,7</sup> Guillaume Viau,<sup>1</sup> Katerina Soulantica,<sup>1</sup> Pierre Fau,<sup>8</sup> Patrick Poveda,<sup>9</sup> Lise-Marie Lacroix,<sup>1\*</sup> Bruno Chaudret<sup>1</sup>

1. Université de Toulouse, UMR 5215 INSA, CNRS, UPS, Laboratoire de Physique et Chimie des Nano-Objets, 135 avenue de Rangueil F-31077 Toulouse cedex 4, France
2. Centre d'Elaboration de Matériaux et d'Etudes Structurales, CEMES-CNRS, 29 rue Jeanne Marvig, B.P. 94347, 31055 Toulouse, France
3. Institut de Physique et Chimie des Matériaux de Strasbourg, Université de Strasbourg, CNRS, UMR 7504, 23 rue du Loess, 67034 Strasbourg, France
4. Department of Physics, CNRS-Ewha International Research Center, Ewha Womans University, Seoul 120-750, South Korea
5. Instituto de Nanociencia de Aragon (INA), Universidad de Zaragoza, Calle Mariano Esquillor, 50018 Zaragoza, Spain
6. ARAID, 50018 Zaragoza, Spain
7. Instituto de Ciencias de Materiales de Aragon, CSIC-U. de Zaragoza, Calle Pedro Cerbuna 12, 50009 Zaragoza, Spain
8. Laboratoire de Chimie de Coordination, UPR 8241, 205 route de Narbonne, 31400 Toulouse, France
9. ST Microelectronics Tours, 10 rue Thalès de Milet, CS 97155, 37071 Tours Cedex 2, France

Corresponding author: [lmacroix@insa-toulouse.fr](mailto:lmacroix@insa-toulouse.fr), Tel: +33567048833, Fax: +33561559697

## Table of content :

<b>Figure S1:</b> TEM images of the different FeCo NPs obtained	2
<b>Figure S2:</b> a) TEM image and b) the corresponding size distribution of FeCo-PA nanocubes.	3
<b>Figure S3:</b> a) TEM image and b) the corresponding size distribution of FeCo-HDAHCl NPs.	3
<b>Figure S4:</b> TEM image of an assembly of FeCo-HDAHCl nanoparticles.	3
<b>Figure S5 :</b> TEM images of FeCo-PA nanocubes after different reaction time	4
<b>Figure S6 :</b> TEM images of FeCo-HDAHCl NPs after different reaction time	4
<b>Figure S7 :</b> XRD pattern of FeCo-HDAHCl and FeCo-PA NPs.	5
<b>Figure S8 :</b> EELS characterization of FeCo-PA NPs.	5
<b>Figure S9 :</b> EELS characterization of FeCo-HDAHCl NPs.	6
<b>Figure S10 :</b> EDX characterization of FeCo-PA and FeCo-HDAHCl NPs.	7
<b>Figure S11 :</b> Mössbauer spectrum recorded at 300K for FeCo-HDAHCl NPs.	7
<b>Table S1 :</b> Mössbauer parameters used for the fitting.	8
<b>Figure S12 :</b> FNR spectrum and the corresponding fit for FeCo-PA NPs.	8
<b>Figure S13 :</b> In situ XRD recorded during thermal annealing of FeCo-PA NPs.	9
<b>Figure S14 :</b> Temperature profile applied for in-situ XRD study.	10
<b>Figure S15 :</b> 5K magnetization curves recorded after field cooling for FeCo-HDAHCl and FeCo-PA NPs.	11
<b>Figure S16 :</b> Additional images of 30 and 60% loaded composite	11
<b>Figure S17 :</b> 300K magnetization curves of FeCo-HDAHCl and 30 and 60% loaded composite.	12
<b>Table S2 :</b> Theoretical and experimental loading in weight percentage of the composite.	12

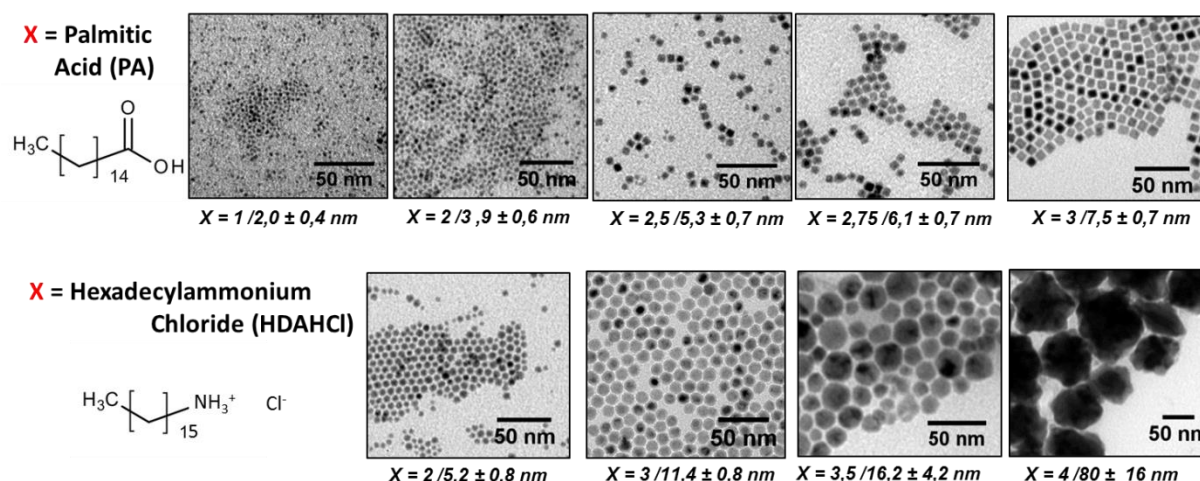


**Figure S1:** TEM images of the different FeCo NPs obtained by varying the nature and the quantity of the acid ( $X$  = Palmitic Acid – PA ; Hexadecylammonium chloride - HDAHCl), while keeping a constant amine concentration (HDA = 4 mmole).  $X=2/3.9\pm0.6 \text{ nm}$  indicates the acid quantity (2 mmole) and the mean size respectively (Gaussian size distribution determined by counting at least 100 nanoparticles).

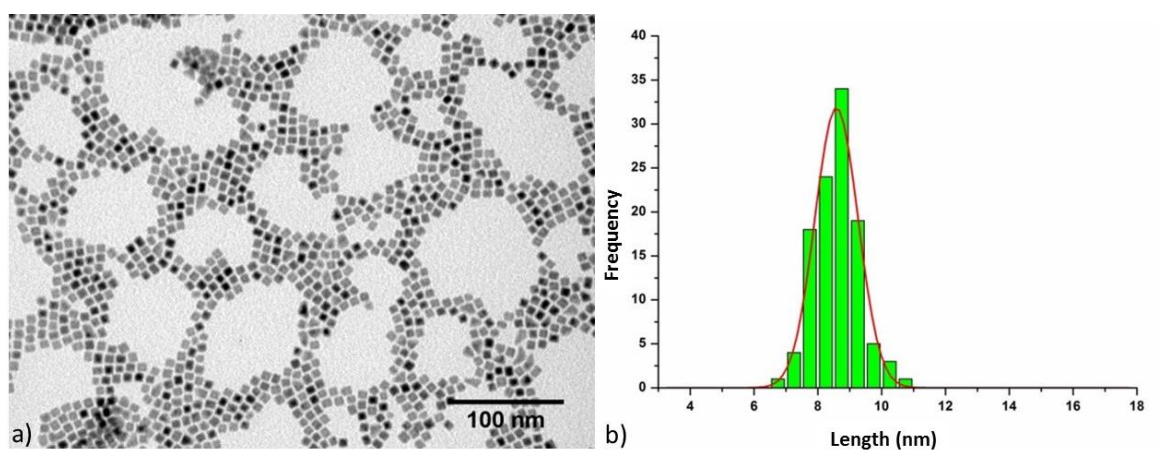


**Figure S2:** a) TEM image and b) the corresponding size distribution of FeCo nanocubes prepared in presence of palmitic acid (PA) and hexadecylamine (HDA) in a 3:4 ratio.

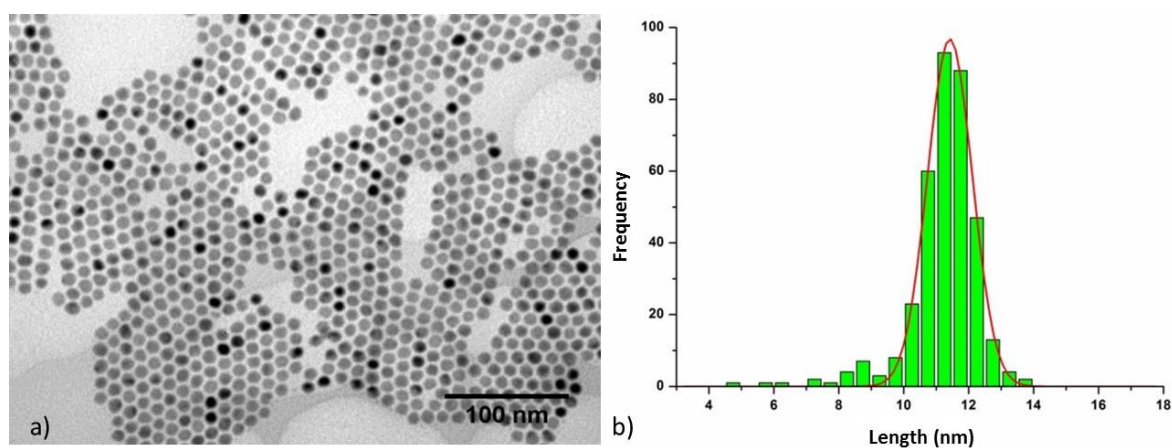


**Figure S3:** a) TEM image and b) the corresponding size distribution of FeCo NPs prepared in presence of hexadecylammonium chloride (HDAHCl) and hexadecylamine (HDA) in a 3:4 ratio.

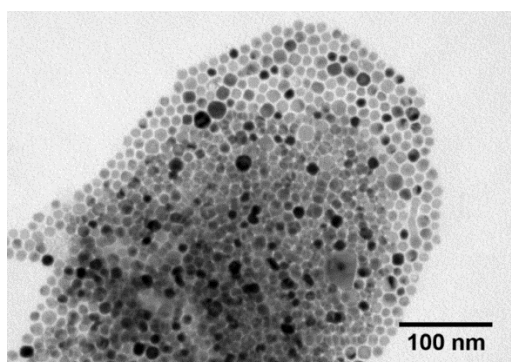


**Figure S4:** TEM image of an assembly of FeCo-HDAHCl nanoparticles.

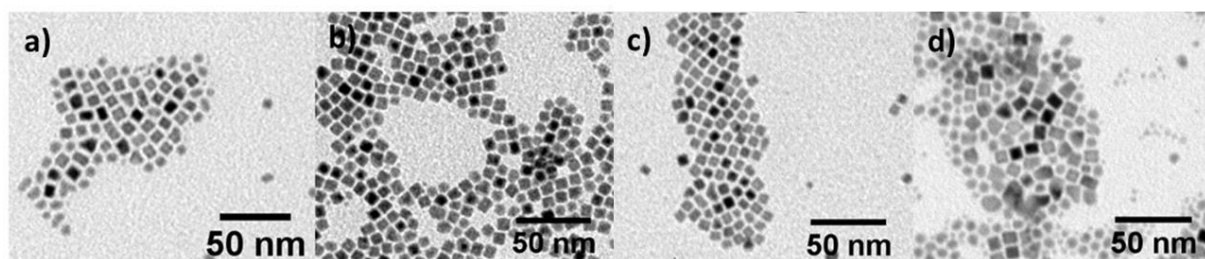


**Figure S5 :** TEM images of FeCo-PA nanocubes obtained after a) 24h, b) 48h, c) 72h and d) 7 day of reaction at 150°C.

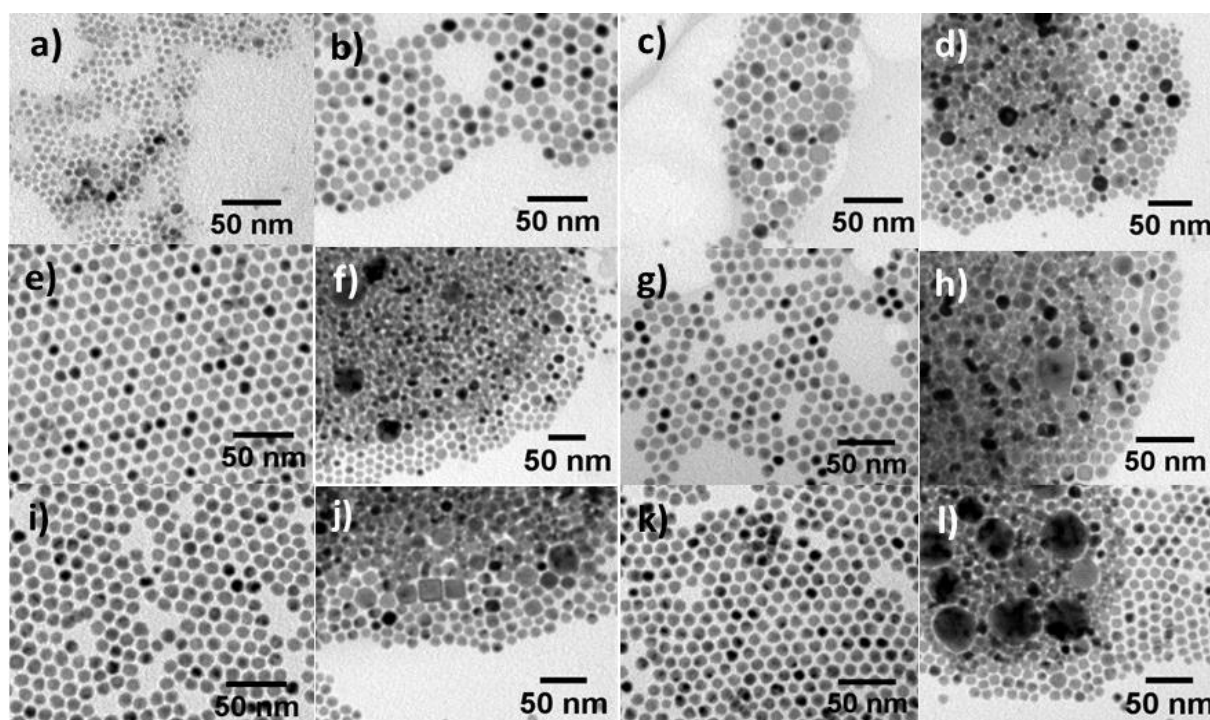


**Figure S6 :** TEM images of FeCo-HDAHCl NPs obtained after a-b) 1h, c-d) 3h, e-f) 6h, g-h) 24h, i-j) 38h and k-l) 48h of reaction at 150°C.



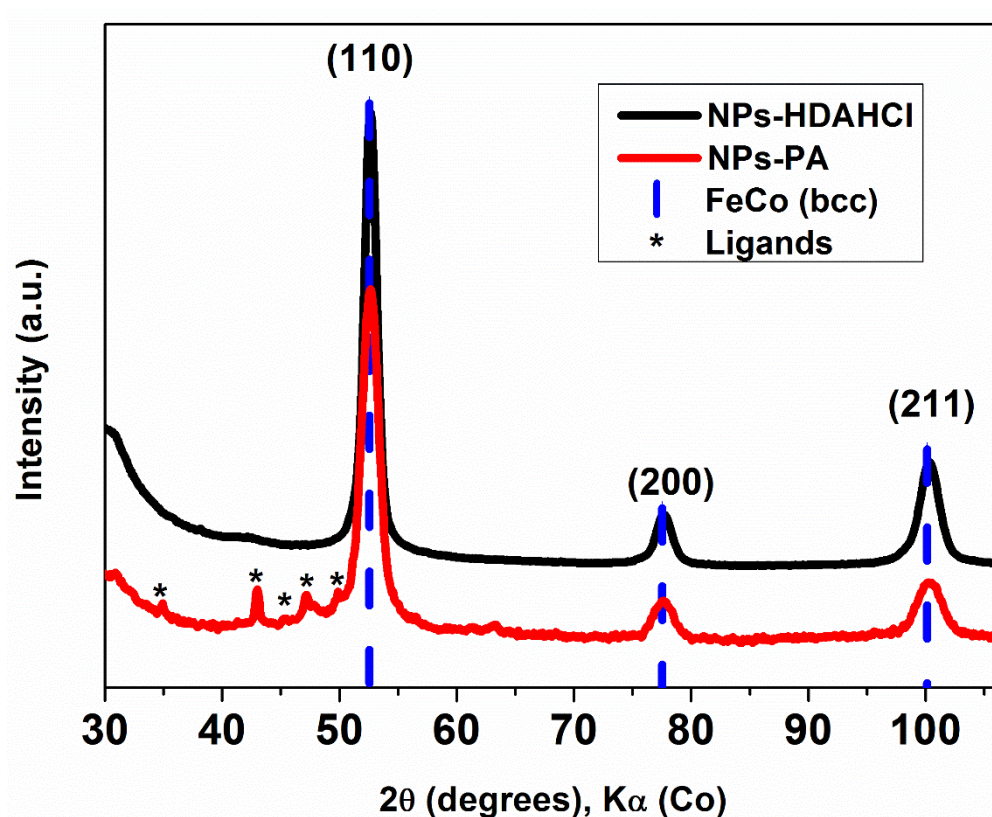


**Figure S7 :** XRD pattern of the FeCo nanoparticles prepared in presence of HDAHCl (black line) or PA (red line), reference pattern (dashed blue line): ICDD # 00-044-1433. Ligand peaks can be attributed to HDA ligands cristallized at the nanocube surface.

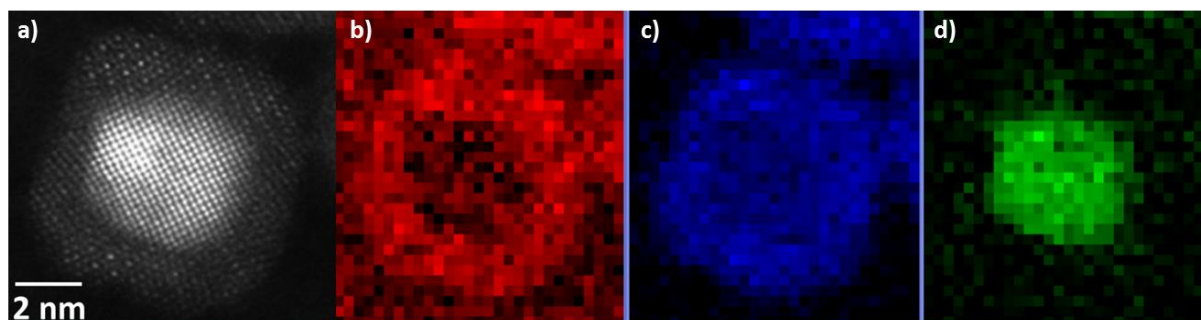


**Figure S8 :** a) Scanning transmission electron microscope (STEM) image using high angle annular dark field detector (HAADF). Chemical mapping obtained by electron energy loss spectroscopy (EELS) showing b) O, c) Fe and d) Co spatial distribution on FeCo NP stabilized with PA ligands.

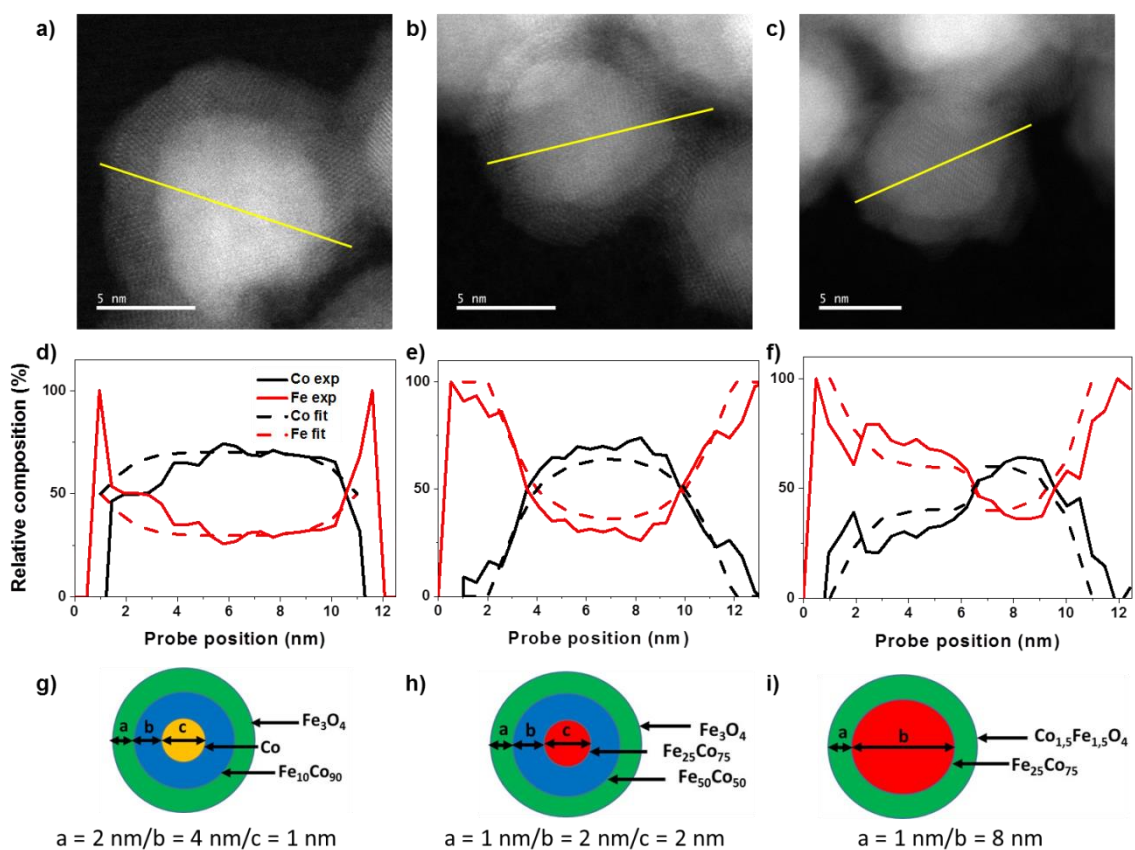


**Figure S9.** a-c) STEM-HAADF images of FeCo-HDAHCl NPs, d-f) relative composition profiles determined by EELS. Experimental (plain line) and simulated (dashed lines) contributions of Co (black and blue respectively) and Fe (red and green respectively). g-i) Models used for the composition simulation corresponding to g) Co-rich core, h) onion-like core and i) FeCo core.

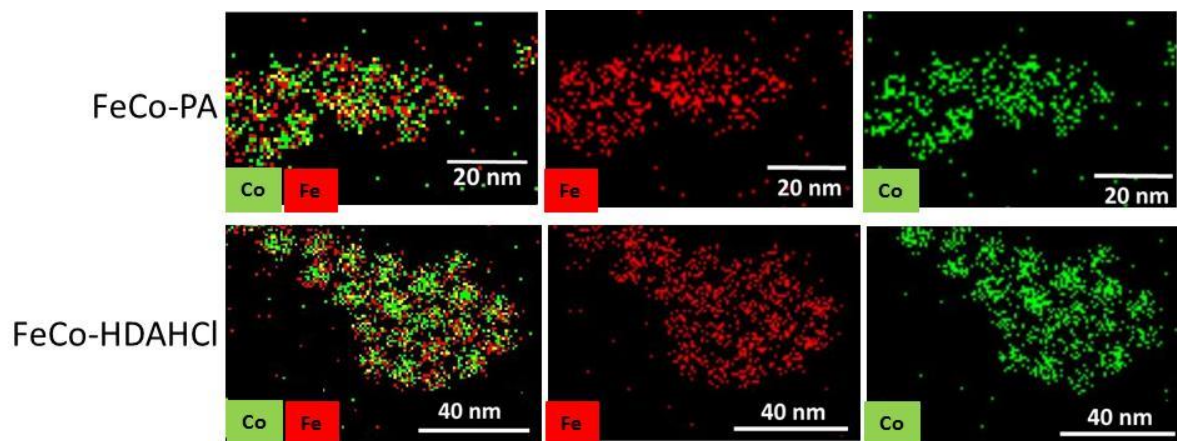


**Figure S10 :** EDX mapping of Fe and Co elements within FeCo NPs prepared in presence of PA (first line) or HDAHCl (second line).

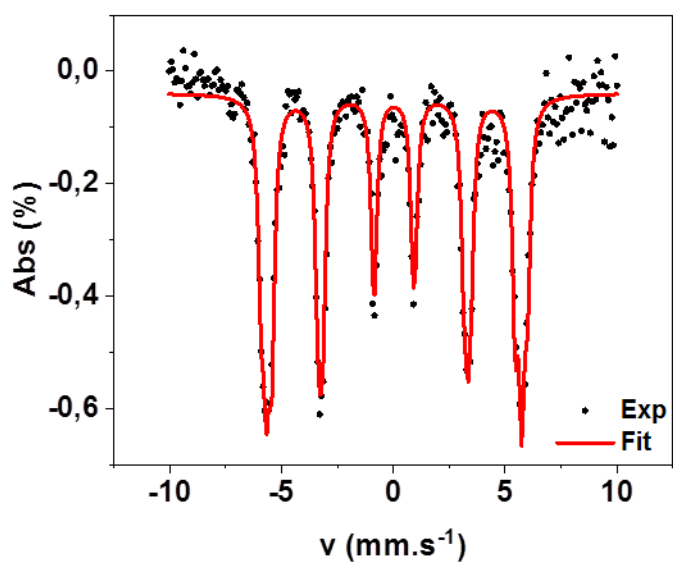


**Figure S11.**  $^{57}\text{Fe}$  Mössbauer spectrum of the FeCo-HDAHCl NPs recorded at 300 K.

**Table S1.** Mössbauer parameters used for the fitting : isomer shift ( $\delta$ ), quadrupole splitting ( $\Delta$ ), hyperfine field (H), full width at maximum height (w). Due to the broad sextet observed, 3 (FeCo-PA) to 4 (FeCo-HDAHCl) individual sextets have been used in the simulation to fit the experimental data. The IV contribution for FeCo-PA NPs corresponds to Fe(II) molecular species magnetically coupled, as previously reported for pure Fe NPs.<sup>1</sup>

Ligands	T (K)	Contribution	$\delta$ (mm/s)	$\Delta$ (mm/s)	H (T)	w	Area (%)
HDAHCl	300	I	0.01	/	33.7	0.15	32
		II	0.01	/	35.0	0.15	9
		III	0.02	/	35.5	0.15	34
		IV	0.04	/	36.9	0.15	25
	5	I	0.14	/	34.1	0.15	22
		II	0.13	/	35.5	0.15	30
		III	0.15	/	36.9	0.15	31
		IV	0.16	/	38.5	0.15	17
PA	5	I	0.1	/	34.4	0.15	26
		II	0.12	/	36.1	0.15	37
		III	0.14	/	37.9	0.15	25
		IV	1.5	-0.3	20.1	0.30	12

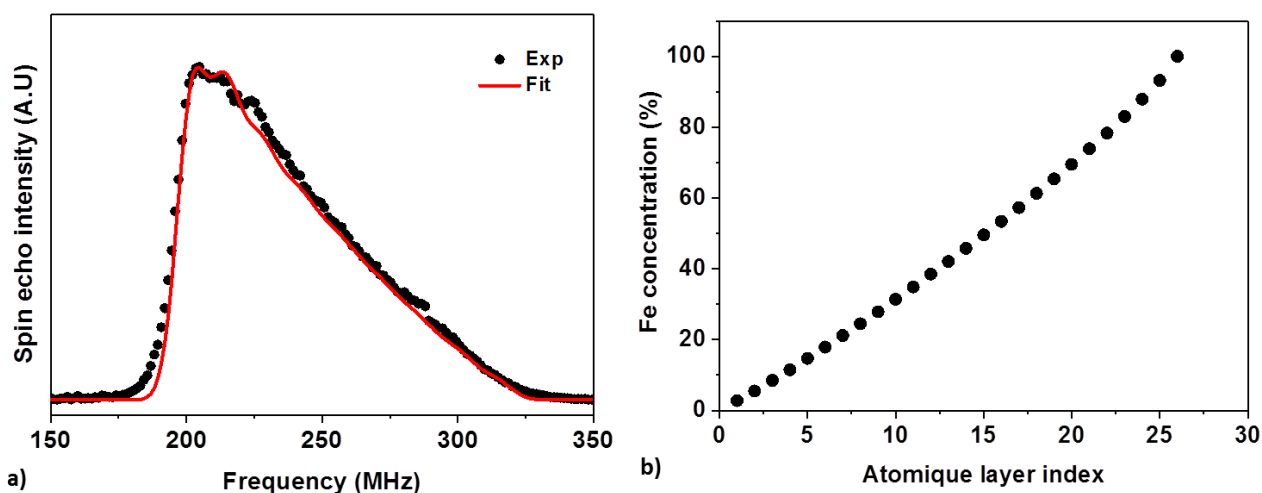


**Figure S12.** a)  $^{59}\text{Co}$  Ferromagnetic Nuclear Resonance of the FeCo-PA NPs recorded at 2K and the corresponding fitting. b) Evolution of the Fe contribution from the NP core to the outer shell as a function of the number of successive atomic layers.



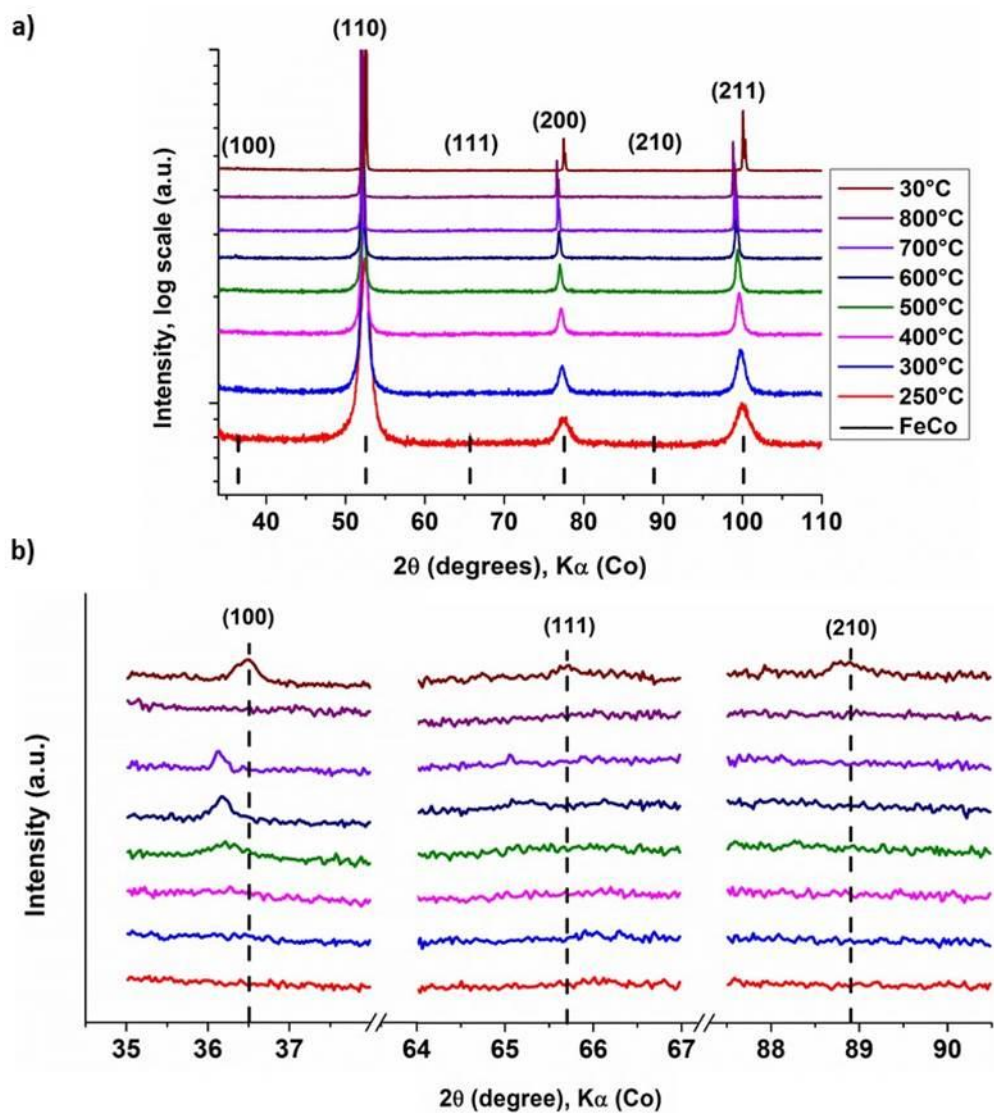


**Figure S13.** a) In-situ XRD recorded during thermal annealing of FeCo-PA NPs under reducing atmosphere. b) Enlarged view of the characteristics B2 superstructures peaks.

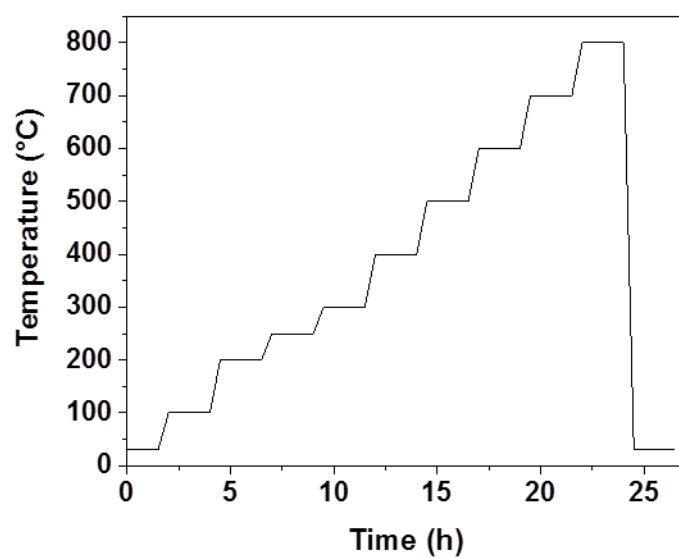


**Figure S14.** Temperature profile followed during the thermal annealing under reducing atmosphere of FeCo-PA NPs. For FeCo-HDAHCl NPs, an additional step at 250°C was introduced to probe the first appearance of the B2 superstructure peaks.

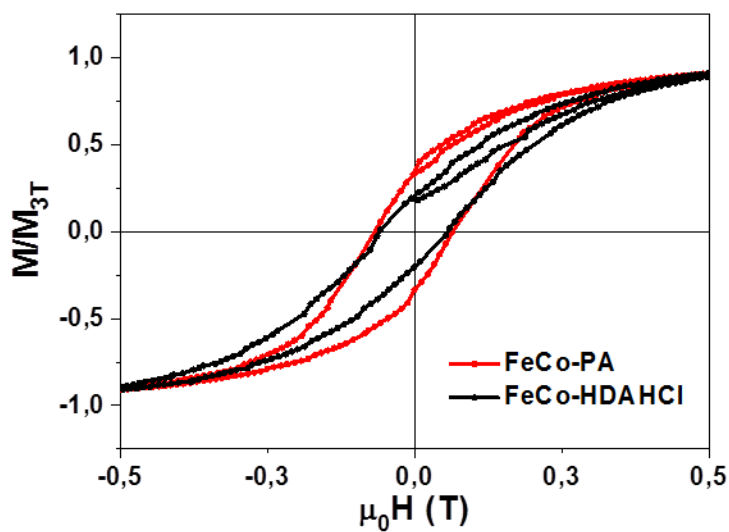


**Figure S15** : Magnetization curve of the FeCo-PA (black) and FeCo-HDAHCl NPs (red) recorded at 5 K after a field cooling ( $\mu_0H = 3T$ )

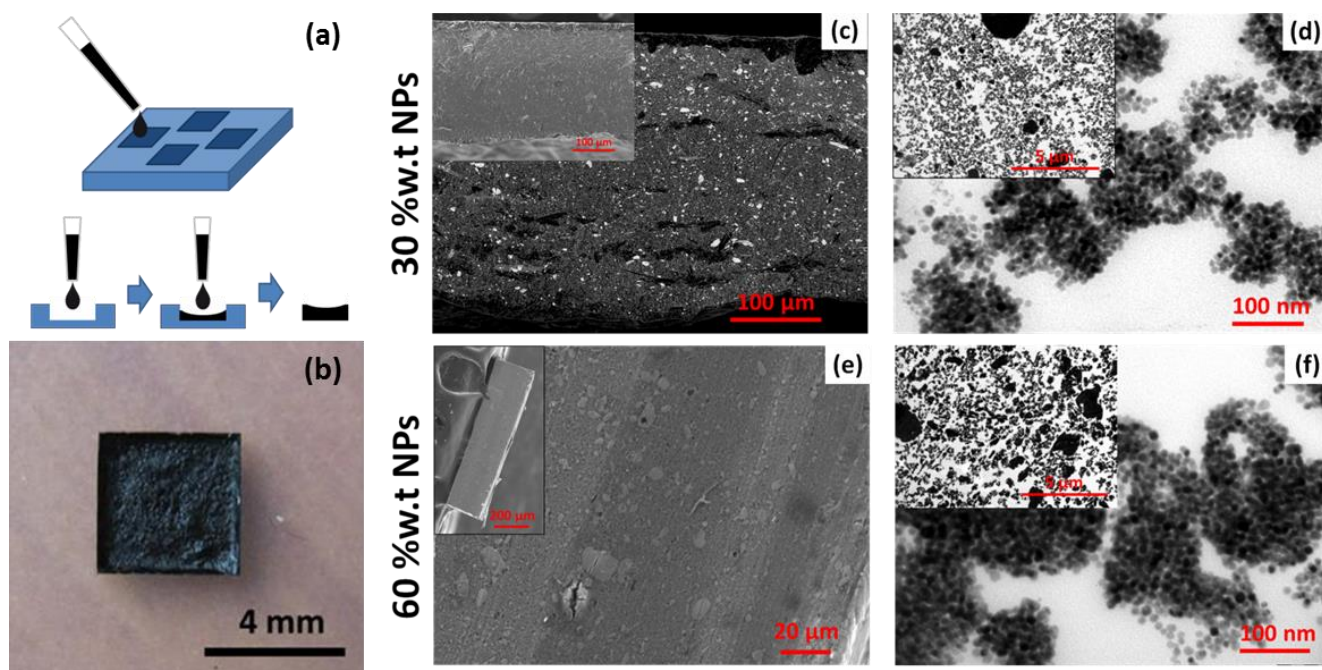


**Figure S16.** a) Schematic view of the pellet preparation and b) the corresponding image. c,e) SEM cross-view image on the pellet thickness and the corresponding d,f) TEM images on pellet'slices prepared by microtomy for c-d)30% and e-f) 60% loaded nanocomposite.

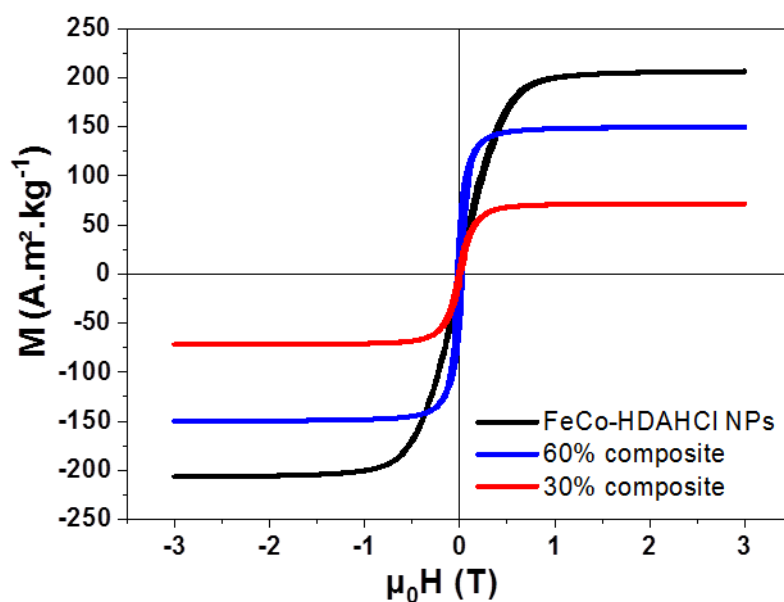


**Figure S17** : Magnetization curves at 300 K of FeCo-HDAHCl NPs (black line) and epoxy composite with a 30% (red line) and 60% (blue line) weight loading.

The nanoparticles weight fraction of the composite was estimated from the magnetization curve with the following expression:

$$\text{Measured weight fraction (\%)} = \frac{M_{3T}}{M_{S_{bulk}} \times m_{Pellet}} \quad (Eq. 1)$$

**Table 2** : Expected loading (calculated from the quantity of FeCo NPs included during the epoxy composite preparation) and experimental loading determined from the magnetization measurement following equation (1)

Theoretical loading (%w.t. FeCo)	10	30	40	47	60
Experimental loading (%w.t. FeCo)	11	34	41	52	62

#### References :

- (1) Lacroix, L.-M.; Lachaize, S.; Falqui, A.; Respaud, M.; Chaudret, B. Iron Nanoparticle Growth in Organic Superstructures. *J. Am. Chem. Soc.* **2009**, *131* (2), 549–557. <https://doi.org/10.1021/ja805719c>.